European Biophysics Journal
https://doi.org/10.1007/s00249-019-01345-8

ORIGINAL ARTICLE

Quantitative characterization of temperature-independent polymer–polymer interaction and temperature-dependent protein–protein and protein–polymer interactions in concentrated polymer solutions

Adedayo A Fodeke[1]

Received: 26 June 2018 / Revised: 24 October 2018 / Accepted: 2 January 2019

Abstract
To study the effect of non-specific interactions arising from proteins being in a crowded environment on physiological processes, the self-interaction of concentrated Dextran T70 and Ficoll 70 and the interactions between a dilute protein and these polymeric macromolecules were quantified using non-ideal tracer sedimentation equilibrium. Sedimentation equilibria of each polymer were measured between 5 and 37 °C, and sedimentation equilibria of 2 mg cm^{-3} superoxide dismutase (SOD) in 0–0.1 g cm^{-3} of each polymer was also measured. Results were analyzed using a model-free thermodynamic virial expression of activity coefficients in terms of the concentration of polymer and a structural model using a statistical thermodynamics approximation. The equilibrium gradients of each of the polymers suggest repulsive interaction, which is independent of temperature. However, the net repulsive interaction between superoxide dismutase (SOD) species and the polymers is dependent on temperature. The ratio of the solvation energy of SOD in Dextran T70 to that in Ficoll 70, $\ln\gamma_{SOD}(Dex)/\ln\gamma_{SOD}(Fic)$ at the same *w/v* concentration was about 1.8 at 37 °C, 1.6 at the intermediate temperature, and ranges from 1.2 to 1.6 at 5 °C over the entire concentration range. The enthalpy and entropy of interaction of SOD with dilute Dextran T70 are − 14 kJ mol^{-1} and − 5.6 J K^{-1} mol^{-1}, respectively. For SOD in dilute Ficoll 70, the enthalpy and entropy are − 8.1 kJ mol^{-1} and 12.9 J K^{-1} mol^{-1}, respectively. Thus, Dextran T70 contributes more to the attractive protein–polymer interaction and to self-association of protein than Ficoll 70 and reasons for this are discussed.

Keywords Macromolecular crowding · Protein–protein interactions · Attractive forces · Ficoll 70 · Dextran T70 · Superoxide dismutase

Introduction

Physiological media are generally characterized by a high total concentration of macromolecules, usually a few hundred mg cm^{-3}, jointly occupying a substantial fraction (0.1–0.4) of the total volume of the medium (Ellis 2001; Zimmerman and Minton 1993; Fulton 1982; Zimmerman and Trach 1991). Such an environment has a considerable biologically significant effect on the rates and equilibria of a broad variety of biochemical associations involving dilute as well as concentrated macromolecular species (Ellis 2001; Minton 2001). Thus, the association state of a particular macromolecule present at low concentration in a medium cannot be reliably inferred from knowledge of the association state of the macromolecule in a solution without other macromolecular components (Minton 2001). Therefore, the characterization of the association state of dilute proteins in the presence of high concentrations of macromolecules presents special challenges to the experimenter over and above those encountered in the study of interactions in dilute solutions. Such challenges in quantification arise from non-specific interactions (both repulsive and attractive) and are due to complications arising from the differences in the nature, size, and structure of the crowding macromolecules.

Two commonly used carbohydrate macromolecular crowders are Ficoll 70 and Dextran T70. Studies of the folding properties of small polypeptides in each of Ficoll

✉ Adedayo A Fodeke
aafodeke@oauife.edu.ng; afodeke@yahoo.co.uk

[1] Department of Chemistry, Obafemi Awolowo University, 200055 Ile-Ife, Nigeria

Published online: 11 January 2019

70 and Dextran T70 showed that crowding with Ficoll 70 resulted in appreciable enhancement in the thermal stability of small peptides in a manner similar to that of large proteins. The rate of protein folding decreased in both Ficoll 70 and Dextran T70. This strange finding shows that, besides an excluded volume effect, other factors might be important in a crowded environment (Mukherjee et al. 2009). These factors are now appreciated, for their impact on hetero- as well as on self-attractive non-specific interaction.

The cellular milieu is composed of several macromolecular components such as proteins, carbohydrates, sugars, nucleic acids, and other solutes. Quantifying non-specific interactions arising from the crowded protein environment is important for the accurate prediction of the role of the medium of protein interaction on its physiological processes (Mukherjee et al. 2009). As a first step in mimicking the cell, it is important to understand binary solutions comprising of a dilute protein in concentrated solutions of an inert protein or carbohydrate polymer crowder. The net repulsive protein–protein, polymer–polymer, and protein–polymer interactions have previously been quantified (Fodeke and Minton 2010, 2011; Jiao et al. 2010).

However, for an adequate understanding of the structural bases of the interaction between the crowders and proteins, a more systematic and comprehensive study of both the attractive and the repulsive interactions between a protein species and each solute component is essential. It is with the aim of accounting for the contributions of the solutes to the interaction between protein and the cellular components that we carried out these studies, which should be useful in predicting the protein behavior in concentrated mixtures.

Significant attractive interactions have been detected between some trace proteins and protein crowders but not in others (Fodeke and Minton 2010, 2011; Jiao et al. 2010). The findings were accounted for in terms of the nature of the surfaces of the interacting proteins. To gauge the free energy of interaction of a single protein in either a protein or carbohydrate crowder at a total concentration in the range of those encountered in living cells, we quantified non-specific interactions of a binary protein–polymer solution, in two single polymer crowders at high polymer concentration. The tracer sedimentation equilibrium technique was used to quantify the interaction of each of the two carbohydrate polymer crowders: Dextran T70, Ficoll 70, and the binary mixture of SOD in arbitrary concentrations of each polymer. The free energy of interaction was determined as a function of the concentration of each polymer at different temperatures. The results were analyzed using a model-free thermodynamic virial expression of activity coefficient in terms of the concentration of polymer and a structural model using a statistical thermodynamics approximation.

Materials and methods

Materials

Ficoll 70 (98% powdered monomer) and Dextran T70 (> 93% purity) were purchased from Sigma-Aldrich (St. Louis, MO, USA). Superoxide dismutase (SOD) (1400 units per mg dry weight) was a product of Worthington Biochemical Corporation, Lakewood, NJ, USA. Fluorescein isothiocyanate (FITC) and Slide-A-Lyzer dialysis cassette (10,000 MWCO) were products of Thermo Scientific, Waltham, MA, USA. SOD, Ficoll 70, and Dextran T70 were all dialyzed extensively against phosphate-buffered saline pH 7.4 before the sedimentation equilibrium experiments. Labeling of SOD and determination of the concentration of Ficoll 70 and SOD were carried out as described previously (Fodeke and Minton 2011). The degree of labeling obtained for SOD was 1 mol of FITC per mol of SOD. Equilibrium sedimentation experiments and gradients analyses were performed as described elsewhere (Fodeke and Minton 2010, 2011; Rosen et al. 2011). The only modification was the adjustment of the rotor speed to 18,000 rpm. This rotor speed was required to attain the equilibrium sedimentation of the mixture.

Methods

Determination of the apparent buoyant molar mass (M^*_{app}) of each of the component protein or carbohydrate polymer at equilibrium sedimentation was carried out as described previously (Darawshe et al. 1993; Fodeke and Minton 2010). M^*_{app} is related to the apparent molar mass, M_{app}, and the density increment $(d\rho/dw)_\mu$ of a species at constant chemical potential, such that M^*_{app} is defined by $M_{app}(d\rho/dw)_\mu$. Density increment values of 0.27 and 0.38 are assumed for SOD and the carbohydrate polymers, respectively (Fodeke and Minton 2010). M^*_{app} of Dextran T70, Ficoll 70, and protein in each polymer were determined from the dependence of the concentration gradient on radial position. For short columns such as were used in the experiment, M^*_{app} was independent of concentration in any particular column. M^*_{app} was determined at least three times for different concentrations of polymer solutions. The dependences of the mean M^*_{app} of the protein and the carbohydrate polymer on the weight per volume (*w/v*) concentration of polymer were analyzed.

Data analysis

Power series expansion of activity coefficients of protein or polymer in terms of polymer concentration and their concentration derivatives

For species in solution (including a single species 1 or species 2, whose apparent buoyant molar mass is determined in a single crowding species 1), the activity coefficient of species 2, γ_2, is related to concentration of species 1 by expansion of the activity coefficient of species 2 in terms of the concentration of species 1 as follows (McMillan and Mayer 1945):

$$\ln \gamma_2 = B_{21} w_1 + B_{211} w_1^2 + B_{2111} w_1^3 + \cdots, \tag{1}$$

where w_1 is the *w/v* concentration of species 1, and B_{21}, B_{211}, and B_{2111} are coefficients of interaction between species 2 and species 1, whose concentrations affect the chemical potential of species 2. In the limit of low concentration, the thermodynamic activity coefficient is linear with crowder concentration, and the first term on the right-hand side of Eq. (1) applies. The terms with B_{211} and B_{2111} become applicable with increasing concentration of solute 1 to high and higher concentrations, respectively.

A special case of Eq. (1) is obtained for the determination of the chemical potential of a single solute species 1 in the absence of species 2 or in the presence of only very trace amount of species 2 when species 2 is not present in sufficient concentration to affect the chemical potential of species 1. Then, the activity coefficient of species 1, whose concentration affects its own chemical potential at sedimentation equilibrium, is given according to

$$\ln \gamma_1 = B_{11} w_1 + B_{111} w_1^2 + B_{1111} w_1^3 + \cdots, \tag{2}$$

where B_{11}, B_{111}, and B_{1111} are coefficients of self-interaction of species 1, whose concentration is sufficiently high to affect its chemical potential. In the limit of low concentration, B_{11} applies. B_{111} and B_{1111} only apply with increasing concentration.

According to the general theory of sedimentation equilibrium, $M^*_{2,\mathrm{app}}$ of a trace solute at sedimentation equilibrium relates to the concentration w_1 of solute 1 and $M^*_{1,\mathrm{app}}$ according to the following (Rivas et al. 1999):

$$M^*_{2,\mathrm{app}} = M^*_2 - w_1 \left(\partial \ln \gamma_2 / \partial w_1 \right) M^*_{1,\mathrm{app}}, \tag{3}$$

where M^*_2 is the buoyant molar mass of species 2 and $\partial \ln \gamma_2 / \partial w_1$ is a measure of interaction between solute species 1 and 2. A net attractive interaction between species 1 and 2 results when the $\partial \ln \gamma_2 / \partial w_1 < 0$. A net repulsive interaction results when $\partial \ln \gamma_2 / \partial w_1 > 0$.

$M^*_{1,\mathrm{app}}$, the apparent buoyant molar mass of species 1 which is the only species that is present in a concentration high enough to affect the chemical potential of the solution mixture is given by

$$M^*_{1,\mathrm{app}} = M^*_1 / \left(1 + B_{11} w_1 + 2 B_{111} w_1^2 + \cdots\right). \tag{4}$$

Equations (1)–(4) were used to fit the experimental data of the dependence of $M^*_{1,\mathrm{app}}$ and $M^*_{2,\mathrm{app}}$ as a function of the concentration of each of the polymers. The B_{11}, B_{111}, B_{21}, and B_{211} terms were obtained from the fitting parameters of the curves of the dependence.

Analysis of SOD–polymer mixture data using scaled particle theory to calculate concentration derivatives of activity coefficients

The model in which polymers and globular proteins are considered as hard convex particles with different structural parameters had previously been used to calculate their activity coefficients. The derivative of the activity coefficient of some globular proteins and Ficoll 70 with respect to the concentration of each species has, therefore, been calculated (Fodeke and Minton 2010, 2011; Darawshe et al. 1993). Here, to analyze the experimental data, two possible weak associations were postulated: One resulting in the formation of a weak hetero-complex between polymer, *P* (Ficoll 70 or Dextran T70), and protein *A* (SOD); the second, self-association of trace protein induced by the presence of the polymer. The interaction between concentrated polymer *P* and trace protein *A*, leading to the formation of a weak hetero-complex, can be represented as follows:

$$A + P \overset{K_{AP}}{\leftrightarrows} AP. \tag{5}$$

The association constant K_{AP} for the formation of hetero-complex *AP* between trace species *A* and crowding polymer *P* measures the extent of the interaction between *A* and *P*.

Weak self-association of trace species *A* induced by concentrated polymer *P* is represented by the equation:

$$P + 2A \overset{K_{A2}}{\leftrightarrows} A_2 + P. \tag{6}$$

The general derivative of activity coefficient of a mixture of convex hard particles in which only a single convex hard particle species is present at a concentration sufficient to affect the chemical potential is given by (Zimmerman and Trach 1991; Labowitz et al. 1965; Boublik 1974)

$$\frac{\partial \ln \gamma_j}{\partial \rho_1} = \frac{V_1}{(1-\rho_1 V_1)} + \left[H_j S_1 + S_j H_1 + V_j\right] \frac{1}{\left(1-\rho_1 V_1\right)^2} + \left[H_j^2 S_1^2 + 2 V_j H_1 S_1\right] \frac{\rho_1}{\left(1-\rho_1 V_1\right)^3} + \left[V_j H_1^2 S_1^2\right] \frac{\rho_1^2}{\left(1-\rho_1 V_1\right)^4}, \quad (7)$$

where ρ_1 is the number density of species 1 which is proportional to concentration w_1 of the polymer. Each of the species is characterized by three shape parameters: the mean radius of curvature H, the surface area S, and the volume of equivalent convex particle V, where the subscript 1 in Eq. (7) denotes polymer and $j=2$ denotes the protein monomer (A), $j=3$ denotes protein–polymer complex (AP), and $j=4$ denotes the protein dimer (A_2). Using the structural model in which the species are treated as hard particles, it is assumed that the volume of the complex AP is given by the sum of the volumes of species A and P and the volume of the A_2 dimer is twice that of species A. Each polymer is treated as a spherocylinder with an axial length-to-diameter ratio of 6.6, and the value previously obtained for Ficoll 70 (Fodeke and Minton 2010). The SOD monomer and dimer are treated as spherical hard particles.

Model for the interaction of SOD with polymer

Three possible types of interaction may result from crowding of SOD (A) by the polymer (P):

1. The equilibrium constant for the self-association of A, induced by an arbitrary concentration of polymer, as described in Eq. (6), is given by

$$K_{A_2} = \frac{C_{A_2}}{C_A^2}, \quad (8)$$

where the subscripts indicate the species involved, and C denote the concentration of each species in mol dm^{-3}.

2. The equilibrium expression for the weak association between SOD and polymer crowder described by Eq. (5) is

$$K_{AP} = \frac{C_{AP}}{\left(C_{P,\mathrm{tot}} - C_{AP}\right)\left(C_{\mathrm{A,tot}} - C_{AP}\right)}. \quad (9)$$

From Eq. (9), it can be shown that

$$\left(C_{A,\mathrm{tot}} - C_{AP}\right) = \frac{C_{A,\mathrm{tot}}}{\left(1 + K_{AP}\left(C_{P,\mathrm{tot}} - C_{AP}\right)\right)}, \quad (10)$$

where $C_{A,\mathrm{tot}}$ and $C_{P,\mathrm{tot}}$ denote the total concentration of SOD and polymer, respectively.

3. A combination of self-association of SOD, induced by the polymer, and an attractive interaction between the polymer and SOD may also occur simultaneously in the protein–polymer binary system.

The equilibrium self-association of A, described in terms of the non-ideality parameters and the concentrations of the species present, is given by

$$K_{A_2} \equiv \frac{C_{A_2}}{C_A^2} = K^{\circ}_{A_2} \frac{\gamma_A^2}{\gamma_{A_2}}. \quad (11)$$

Similarly, the hetero-association equilibrium constant may be related to the applicable non-ideality parameters by

$$K_{AP} \equiv \frac{C_{AP}}{C_A C_P} = K^{\circ}_{AP} \frac{\gamma_A \gamma_P}{\gamma_{AP}}, \quad (12)$$

where $K^{\circ}_{A_2}$ and K°_{AP} are, respectively, the protein self-association and the protein–polymer hetero-association constants at infinite dilution and γ_A, γ_P, γ_{A_2}, and γ_{AP} describe the non-ideality parameters of species given as subscripts. Since C_A is much less than C_P, a valid assumption is that, even at its maximum, the concentration of AP is much smaller than the concentration of P, so that in Eq. (10), $C_{P,\mathrm{tot}}$–$C_{\mathrm{Ap}} \approx C_{P,\mathrm{tot}}$ (the input variable). From the conservation of mass condition

$$C_{A,\mathrm{tot}} = C_A + 2C_{A_2} + C_{AP} = C_A + 2K_{A_2} C_A^2 + K_{AP} C_A C_{P,\mathrm{tot}}. \quad (13)$$

Equation (13) was analytically solved for C_A as a function of $C_{P,\mathrm{tot}}$, $C_{A,\mathrm{tot}}$, K_{A_2}, and K_{AP}. The last two terms are functions of $K^{\circ}_{A_2}$ and K°_{AP}, respectively, and are determined with Eqs. (3), (11), and (12) using the fitted structural parameters of the protein and polymer in Eq. (7).

Statistical analyses of the experimental data using approximate structural hard particle model assuming three different types of interaction

In the statistical thermodynamic model I, all 39 experimental data points of the four experimental data sets were fitted simultaneously with respect to the variation of six fitting structural parameters, including the effective specific volume of SOD ($V_{\mathrm{eff},A}$) and the effective specific volume of polymer ($V_{\mathrm{eff},P}$), $K^{\circ}_{A_2}$ at 5 °C, and K°_{AP} at the three temperatures of the experiment. In statistical thermodynamic model II, the four experimental data sets were fitted simultaneously with the parameters in model I, except $K^{\circ}_{A_2}$ at 5 °C. In the statistical thermodynamic model III, the variation of two additional fitting parameters ($K^{\circ}_{A_2}$ at 25 °C and 37 °C) was allowed, in

addition to those of model I, in fitting the curve to the experimental data. The ratio of the sum of squared residuals of the data of each of the structural models I–III fit to that of virial expansion fit was determined in each case and compared to the critical value of F for the degree of freedom of the relevant data at the 95% confidence limit. Given the concentrations of all species in the solution, as well as the derivative of the natural logarithm of their activity coefficients with respect to the concentration of the crowder, M^*_{app} of both the crowder and the tracer may be calculated as a function of w_P using Eq. (3) (Rivas et al. 1999; Zorrilla et al. 2004). With the estimation of K°_{AP} at different temperatures, it becomes possible to determine the enthalpy and entropy of the polymer–protein interaction at infinite dilution, using the van't Hoff equation:

$$\ln K^{\circ}_{AP}(T) = -\frac{\Delta G^{\circ}}{RT} = -\frac{\Delta H^{\circ}}{RT}\left(\frac{1}{T}\right) + \frac{\Delta S^{\circ}}{RT}. \quad (14)$$

Results

Dextran T70 and Trace SOD in Dextran T70

Figure 1a presents data set 1, the experimental data for the dependence of $M^*_{app,Dex}$ on the concentration of Dextran T70, w_{Dex}, at 5 °C, 27 °C, and 37 °C. Within the experimental uncertainty, the dependence of $M^*_{app,Dex}$ on w_{Dex} is independent of temperature in the range 5–37 °C. Data sets 2, 3, and 4 plotted in Fig. 1b show the dependence of $M^*_{app,SOD}$ on w_{Dex} at 5, 27, and 37 °C, respectively. It can be seen that the dependence of $M^*_{app,SOD}$ on w_{Dex} is sensitive to temperature. All four data sets were modeled simultaneously to obtain the best-fit curves of the model equations by minimizing the sum of the squared residuals (SSR) with respect to the variation of a single set of fitting parameters. In all the data sets described by the effective hard particle model, Dextran T70 denoted by D is species 1 and SOD denoted by S is species 2. The Dextran–SOD hetero-complex, SD, and the SOD dimer, S_2, are species 3 and 4, respectively. The best-fit parameter values and the best-fit SSR obtained from fitting the virial expansion formulation are presented in Table 1 (column 1). The best-fit parameters of the effective hard particle model permitting SOD dimerization at 5 °C and hetero-association at all temperatures (statistical thermodynamic model I) are presented in Table 1 (column 2). Table 1 (column 3) presents the best-fit parameters of the hard particle model when only hetero-association was allowed (statistical thermodynamic model II). The black curve in Fig. 1a is the curve fitted through the data with Eq. (4). The black curves of Fig. 1b were calculated using Eq. (3) and the derivative of Eq. (1) with respect to w_{Dex} together with the temperature-dependent fitting parameters, as reported in Table 1 (column 1). The blue curves plotted alongside for comparison were calculated using Eqs. (3), (7), and (11)–(13) of the approximate hard particle model, together with the fitting parameters, as reported in Table 1 (column 2). The SSR values are presented to show the goodness of the fit of the structural model compared to the virial expansion fit. The F test showed that the calculated curve

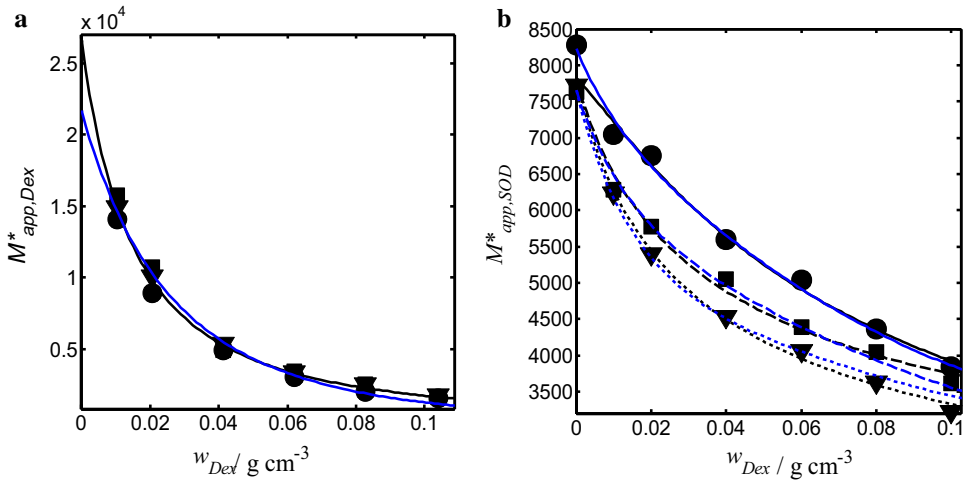

Fig. 1 Dependence of apparent buoyant molar mass of: **a** Dextran T70 on *w/v* concentration of Dextran T70; **b** SOD on *w/v* concentration of Dextran T70. Symbols: circles, 5 °C; squares, 27 °C; triangle, 37 °C. In **a**, the black curve is the fit of the experimental data with virial Eq. (4); the blue curve is the fit of the experimental data to the convex hard particle model equation, as described in the text. **b** Black curves are fits of the experimental data with virial Eq. (3) together with the temperature-dependent coefficient of interaction in Table 1 (column 1). Blue curves are those calculated using the structural parameters of the convex hard particle model, as described in the text. Curve description of **b**: 5 °C, full curve; 27 °C, broken curve; and 37 °C, dotted curve. Each experimental data point is the mean of at least two replicate experiments and is subject to a standard error of about 5%

Table 1 Fitting parameters for the data on the interaction of Dextran T70 molecules and Dextran T70 with SOD in a binary mixture of SOD and Dextran T70

Virial expansion model	Statistical thermodynamic model I	Statistical thermodynamic model II
$M^*_D = 26{,}600$	$M^*_D = 21{,}643\ (-424, +880)$	$M^*_D = 21{,}601$
$M^*_S = 7824$	$M^*_S = 7837\ (-63, +39)$	$M^*_S = 7815$
$B_{11} = 67.8477$	$V_{\mathrm{eff},S} = 1.55\ (-0.05, +0.07)$	$V_{\mathrm{eff},S} = 1.56$
$B_{111} = 363.7592$	$V_{\mathrm{eff},D} = 2.01\ (-0.15, +0.05)$	$V_{\mathrm{eff},D} = 2.00$
$B_{21}(5\ ^\circ\mathrm{C}) = 1.95$	$\log K^\circ_{S_2}(5\ ^\circ\mathrm{C}) = 2.23\ (-0.71, +0.29)$	$\log K^\circ_{S_2}(5\ ^\circ\mathrm{C}) = 0$
$B_{211}(5\ ^\circ\mathrm{C}) = 100.74$	$\log K^\circ_{S_2}(27\ ^\circ\mathrm{C}) = 0$	$\log K^\circ_{S_2}(27\ ^\circ\mathrm{C}) = 0$
$B_{21}(25\ ^\circ\mathrm{C}) = 7.07$	$\log K^\circ_{S_2}(37\ ^\circ\mathrm{C}) = 0$	$\log K^\circ_{S_2}(37\ ^\circ\mathrm{C}) = 0$
$B_{211}(25\ ^\circ\mathrm{C}) = 80.21$	$\log K^\circ_{SD}(5\ ^\circ\mathrm{C}) = 2.30\ (-0.12, +0.08)$	$\log K^\circ_{SD}(5\ ^\circ\mathrm{C}) = 2.34$
$B_{21}(37\ ^\circ\mathrm{C}) = 8.48$	$\log K^\circ_{SD}(27\ ^\circ\mathrm{C}) = 2.14\ (-0.10, +0.07)$	$\log K^\circ_{SD}(27\ ^\circ\mathrm{C}) = 2.09$
$B_{211}(37\ ^\circ\mathrm{C}) = 84.79$	$\log K^\circ_{SD}(37\ ^\circ\mathrm{C}) = 1.97\ (-0.04, +0.03)$	$\log K^\circ_{SD}(37\ ^\circ\mathrm{C}) = 1.90$
$\mathrm{SSR} \times 10^{-8} = 0.92$	$\mathrm{SSR} \times 10^{-8} = 1.20$	$\mathrm{SSR} \times 10^{-8} = 1.70$

Subscripts in parameter names: $1 = D$ for Dextran T70; $2 = S$ for SOD. Values of B_{11}, or B_{21}, and B_{111} or B_{211} are in $\mathrm{cm^3\ g^{-1}}$ and $\mathrm{cm^6\ g^{-2}}$, respectively. SSR is the sum of squared residuals of the experimental data to the fitted curve. Specific excluded volumes $V_{\mathrm{eff},S}$ and $V_{\mathrm{eff},D}$ are in $\mathrm{cm^3\ g^{-1}}$ and M^*_D and M^*_S are in $\mathrm{g\ mol^{-1}}$. K°_{SD} and $K^\circ_{S_2}$ are given in $\mathrm{dm^3\ mol^{-1}}$

of the dependence of $M^*_{\mathrm{app,SOD}}$ on w_{Dex} using the parameters of Table 1 (column 2) (structural model I) is identical to the curve of the virial expansion fit to the data within the 95% confidence limit. However, the curve fitted to the experimental data with structural model II (not shown) is significantly different from that fitted with the virial expansion model. Model I was, therefore, considered appropriate for the description of the interaction of SOD with Dextran T70 under the conditions of the experiment.

Ficoll 70 and Trace SOD in Ficoll 70

The dependence of M^*_{appFic} on w_{Fic} at 5, 25, and 37 °C (data set 1) is presented in Fig. 2a. The data are identical to those reported previously and are independent of temperature within the experimental uncertainty of the measurements (Fodeke and Minton 2010). The black curve through the data points was calculated using the virial expansion (truncated at the quadratic term) of the activity coefficient in terms of the concentration of Ficoll 70. The blue curve, calculated with the best-fit values of M^*_{Fic} and $V_{\mathrm{eff},F}$ using the convex hard particle model, Table 2 (column 3), was plotted, for comparison, together with the black curve of the virial expansion model, as described in the previous section. Figure 2b presents data sets 2, 3, and 4 of the dependence of $M^*_{\mathrm{app,SOD}}$ on w_{Fic} at 5, 25, and 37 °C, respectively. All four data sets of Fig. 2a, b were modeled simultaneously to obtain the best fit of the model Eqs. (3) and (7). Fitting was done by minimizing the total sum of squared residuals with respect to the variation of a single set of the fitting parameters in Table 2 (column 1) for virial fit (black curves in Fig. 2) and Table 2 (column 3) for the structural model fit (blue curves of Fig. 2). In all the data sets for the effective hard particle model, Ficoll 70, denoted by F, is species 1; SOD, denoted by S, is species 2; SOD–Ficoll 70 heterocomplex, denoted by SF, is species 3, and species 4 is the SOD dimer, denoted by S_2. In Fig. 2b, it is seen that the experimental data point of $M^*_{\mathrm{app,SOD}}$ at a given w_{Fic} is

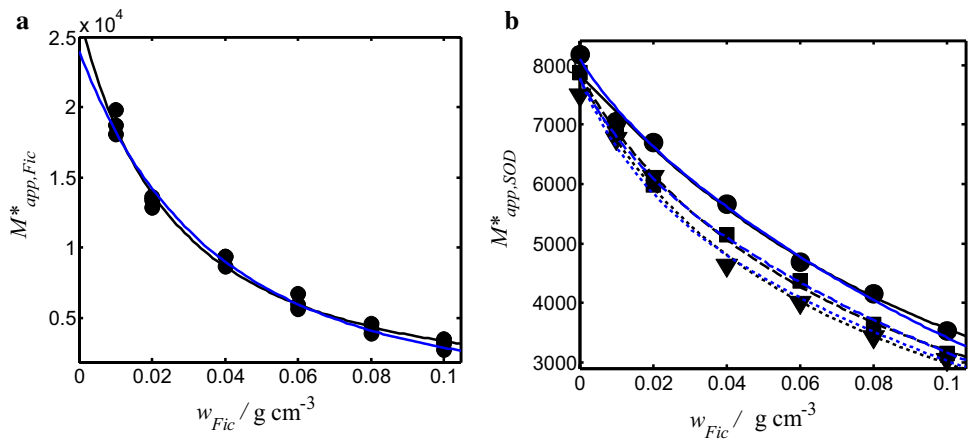

Fig. 2 Dependence of apparent buoyant molar mass of: **a** Ficoll 70 on concentration (*w/v*) of Ficoll 70; **b** SOD on concentration (*w/v*) of Ficoll 70. The square symbol and broken curve describe data at 25 °C. Other temperature symbols and curve types are described in Fig. 1

Table 2 Fitting parameters to the data for interaction of Ficoll 70 and for interaction in a binary mixture of SOD and Ficoll 70

Virial expansion model	Statistical thermodynamic model I	Statistical thermodynamic model II
$M^*_F = 26{,}600$	$M^*_F = 22{,}997\ (-3215, +3958)$	$M^*_F = 22{,}995 \pm 2000$
$M^*_S = 7837$	$M^*_S = 7755\ (-172, +222)$	$M^*_S = 7874 \pm 500$
$B_{11} = 40.14$	$V_{\mathrm{eff},S} = 1.50\ (-0.05, +0.07)$	$V_{\mathrm{eff},S} = 1.50 \pm 0.10$
$B_{111} = 148.50$	$V_{\mathrm{eff},F} = 2.01\ (-0.48, +0.19)$	$V_{\mathrm{eff},F} = 1.32 \pm 0.20$
$B_{21}(5\ ^\circ\mathrm{C}) = 2.30$	$\log K^\circ_{S_2}(5\ ^\circ\mathrm{C}) = 1.97(-\infty, +0.40)$	$\log K^\circ_{S_2}(5\ ^\circ\mathrm{C}) = 0$
$B_{211}(5\ ^\circ\mathrm{C}) = 148.50$	$\log K^\circ_{S_2}(25\ ^\circ\mathrm{C}) = 0$	$\log K^\circ_{S_2}(25\ ^\circ\mathrm{C}) = 0$
$B_{21}(25\ ^\circ\mathrm{C}) = 2.30$	$\log K^\circ_{S_2}(37\ ^\circ\mathrm{C}) = 0$	$\log K^\circ_{S_2}(37\ ^\circ\mathrm{C}) = 0$
$B_{211}(25\ ^\circ\mathrm{C}) = 52.65$	$\log K^\circ_{SF}(5\ ^\circ\mathrm{C}) = 2.19(-0.09, +0.15)$	$\log K^\circ_{SF}(5\ ^\circ\mathrm{C}) = 2.20 \pm 0.10$
$B_{21}(37\ ^\circ\mathrm{C}) = 4.91$	$\log K^\circ_{SF}(25\ ^\circ\mathrm{C}) = 2.09(-0.05, +0.13)$	$\log K^\circ_{SF}(25\ ^\circ\mathrm{C}) = 2.07 \pm 0.07$
$B_{211}(37\ ^\circ\mathrm{C}) = 48.28$	$\log K^\circ_{SF}(37\ ^\circ\mathrm{C}) = 2.01(-0.06, +0.14)$	$\log K^\circ_{SF}(37\ ^\circ\mathrm{C}) = 1.98 \pm 0.07$
$\mathrm{SSR} \times 10^{-7} = 4.9$	$\mathrm{SSR} \times 10^{-7} = 4.9$	$\mathrm{SSR} \times 10^{-7} = 5.5$

Subscript F symbolizes Ficoll 70. Other subscript symbols and units are in Table 1

dependent on temperature. The fitting parameters of interaction, B_{21} and B_{211}, were, therefore, allowed to vary with temperature in the virial expansion model. In the structural hard particle model, the values of K°_{SF} were also allowed to vary with temperature. The F test showed that the curve of the structural model II, in which only the equilibrium constant of hetero-association was allowed to vary, was identical with the virial fit within 95% confidence limit. The variation of $K^\circ_{S_2}$ at 5 °C in addition to K°_{SF} (not shown) results in no significant improvement of the fit and gave a $V_{\mathrm{eff},F}$ value of 2.01 $\mathrm{cm^3\ g^{-1}}$. This value is considered unreasonable, as it is inconsistent with the value 1.32 $\mathrm{cm^3\ g^{-1}}$ previously obtained for Ficoll 70 (Fodeke and Minton 2010). Therefore, under the experimental conditions, model I was discarded, and model II was considered adequate for describing the interaction of SOD with Ficoll 70.

Discussion

Polymer–polymer interaction

F tests comparing the black curve through the Dextran T70 data with the blue curve (Fig. 1a), and the black curve through the Ficoll 70 data with the blue curve (Fig. 2a), show that the fit of the convex hard particle model to the experimental data for Ficoll 70 is better than the fit to the Dextran T70 data. This indicates that Ficoll 70 fits better to the hard particle model than Dextran T70. Visual inspection shows that the fit of the Dextran T70 data to the hard particle model is particularly poor at low w_{Dex} (compare Figs. 1a and 2a). In the low concentration range, where the Dextran T70 solution is expected to behave ideally, we postulate that this is not so due to the long-range repulsive interactions between the Dextran T70 molecules. This lowers the value of $M^*_{\mathrm{app,Dex}}$ under the dilute conditions than if Dextran T70 was a compact hard particle. This may be the consequence of a more expanded nature of Dextran T70 molecules at low concentrations. In spite of the weakness of the structural hard particle model in fitting the Dextran T70 data, it is interesting to note that it is able to account for some structural features of the interaction of Dextran T70. Ficoll 70 and Dextran T70 have about the same molecular weight and are expected to have identical excluded volumes if both molecules were equally compact. The average specific volume of Dextran T70 obtained from the fit of the experimental data to the structural model is 2.01 $\mathrm{cm^3\ g^{-1}}$, whereas that of Ficoll 70 is 1.32 $\mathrm{cm^3\ g^{-1}}$. This suggests that Dextran T70, in addition to having a hardcore, might possess a somewhat soft network of an elastic structure, whose size decreases with increasing w_{Dex}. This soft, elastic structure is particularly important at low concentrations of Dextran T70 and might be responsible for the observed deviation of $M^*_{\mathrm{app,Dex}}$ from the value expected for a hard particle at very low concentrations when Dextran T70 is treated as a hard convex particle. With increasing concentration of Dextran T70, as crowding increases, the molecules become more compact and approach the model of a hard particle and resistance to further compression becomes significant. At these high concentrations, the hard particle model becomes more valid for the description of the Dextran T70 structure, hence the improvement in the goodness of the fit to the hard particle model with increasing Dextran T70 concentrations (Fig. 1b).

The minimum ratio of the model-independent activity coefficients of the polymers, $\ln\gamma_{\mathrm{Dex}}/\ln\gamma_{\mathrm{Fic}}$ estimated from Fig. 3a is 1.7 at low concentrations. This value increases with increasing polymer concentration to a maximum value of 1.9 at the highest concentration. This indicates that the excess free energy for the insertion of a single Dextran T70 molecule (in arbitrary w_{Dex}) is about 1.8 times that of Ficoll 70 at the equivalent concentration. This ratio was determined using Eq. (2), truncated at the quadratic term with the fitting parameters in Table 1 (column 1). Two possible justifications

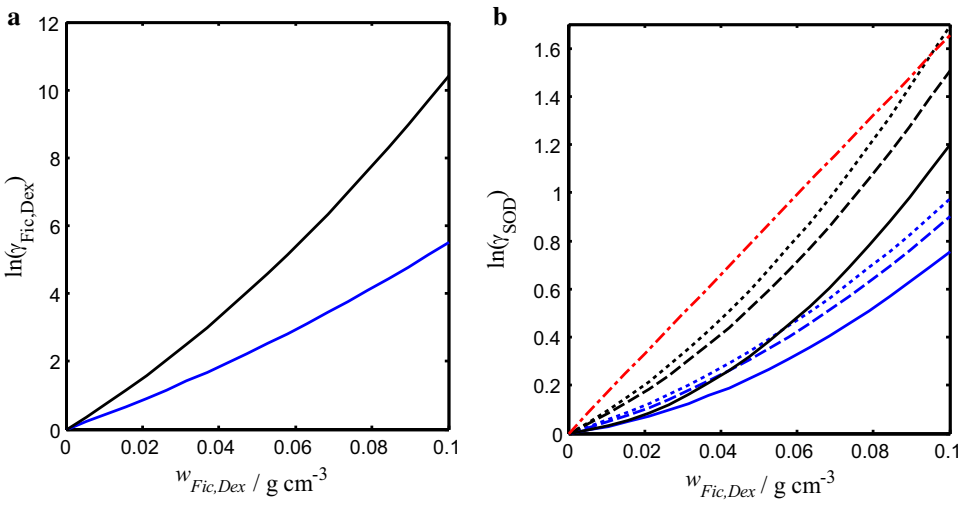

Fig. 3 Dependence of the energy of solvation of **a** Dextran T70 molecules on Dextran T70 concentration (black curve), Ficoll 70 molecules on Ficoll 70 concentration (blue curve), **b** SOD on concentration of Ficoll 70 (blue curves; full—5 °C, broken—25 °C, and dotted—37 °C) and Dextran T70 (black curves; full—5 °C, broken—27 °C, and dotted—37 °C). The broken-dotted red line was calculated for Dextran T70 with the temperature-independent Ogston model Eq. (17), based on the expected excluded volume (neglecting attractive interactions)

might be considered for the difference: (1) the number density of Dextran T70 is greater than that of Ficoll 70 in solutions of identical *w/v* concentration or (2) Dextran T70 has a more extended structure in solution than Ficoll 70. The former consideration is illogical, since the estimated molar masses of Ficoll 70 and Dextran T70 are quite comparable, and their molecules are expected to have comparable number densities at the same *w/v* concentrations. Within experimental error, it is improbable that the difference in molar mass of ca. 3500 g mol^{-1} between Ficoll 70 and Dextran T70 could account for the difference of $0.8\Delta\Delta G_{solv}/RT$ excess free energy of Dextran T70 above that of Ficoll 70. Comparison of the effective volume of Dextran T70 with that of Ficoll 70, as estimated from the scaled particle model, shows that Dextran T70 is a more extended molecule compared to Ficoll 70: $V_{eff,Dex}/V_{eff,Fic} \approx 1.52$. This suggests that the extended nature of Dextran T70 might be the reason for the higher solvation energy of Dextran T70 compared to that of Ficoll 70. Extra work has to be done to make space for another Dextran T70 molecule in Dextran T70 solution compared to that needed to make space for a Ficoll 70 molecule in a Ficoll 70 solution of equivalent concentration.

SOD–polymer interaction

Quantitative characterizations of composition and temperature dependences of the interaction between SOD and carbohydrate polymers were carried out with two major objectives: first, to compare two of the commonly used crowders (Ficoll 70 and Dextran T70) with a view to accounting quantitatively, or at least semi-quantitatively, for any differences in their interaction with trace SOD and Second, to determine the nature of the interaction induced between the trace protein molecules, on one hand, and between the trace protein and polymer molecules on the other hand. To achieve these goals, the excess free energies of insertion of a single SOD molecule in an arbitrary concentration of each polymer were computed at different temperatures using Eq. (1) truncated at the quadratic term (Fig. 3b). The temperature-dependent coefficients of the interaction of SOD with each polymer, B_{21} and B_{211}, at applicable temperatures reported in Tables 1 and 2 were used.

Ogston model and SOD–Dextran T70 interaction

The excluded volume contribution to the interaction between SOD and Dextran T70 is given by the Ogston available volume theory (Minton 1983; Ogston 1958, 1970; Homouz et al. 2008):

$$\ln\gamma_{excluded} = \left(1 + \frac{r_s}{r_p}\right)^2 v_{ex,p}\, w_p. \tag{17}$$

In Eq. (17), r_s and r_p are the radii of equivalent spherical particles of SOD and Dextran T70, respectively, and $v_{ex,p}$ and w_p are the effective excluded volume and *w/v* concentration of Dextran T70 respectively. Values of 0.75 cm^3 g^{-1} and 0.70 nm were set for $v_{ex,p}$ and r_p. These values were obtained from the previous analyses of Dextran T70 experimental

Table 3 Structural and thermodynamic parameters calculated from the best-fit values of curves to the data reported in Figs. 1, 2, and 3

Polymer	$r_{Polymer}$ (nm)[a]	r_{SOD} (nm)[a]	$h_{Polymer}$ (nm)[a]	ΔH_{SOD} (kJ mol^{-1})[b]	ΔS_{SOD} (J K^{-1} mol^{-1})[b]
Dextran T70	0.7	2.59	–	− 14	− 5.6
Ficoll 70	1.45	2.59	19.09	− 8.1	12.9

Superscript symbols: a, calculated from applicable data in column 2 of Table 1 and column 3 of Table 2; b, calculated from Fig. 4

data using the Ogston available volume theory (Jiao et al. 2010; Rivas et al. 1999; Laurent and Killander 1964). The value of r_s was set equal to the value obtained by calculating the radius of the effective volume obtained from fitting the dependence of $M^*_{app,SOD}$ on w_{Fic} to the hard sphere model (Table 3). It makes sense to use this value because essentially the same value was obtained for the effective volume of SOD in BSA earlier (Fodeke and Minton 2011), though no significant attractive interaction was identifiable between SOD and BSA (Fodeke and Minton 2011). In Table 3, $h_{polymer}$ denotes the cylindrical height of the spherocylindrical polymer.

It is noteworthy that the determination of the fitting parameters used in calculating the excess free energy values of the curve (Fig. 3) is independent of any model of molecular structure or intermolecular interaction. Unlike the Ogston model that assumes only excluded volume, the excess free energy calculated from the temperature-dependent value for B_{21} and B_{211} account for both attractive and excluded volume interactions. Estimation of the ratio of the solvation energy of SOD in Dextran T70 to the solvation energy of SOD in Ficoll 70, $\ln\gamma_{SOD}(Dex)/\ln\gamma_{SOD}(Fic)$, shows that at both intermediate and high temperatures, in the limit of experimental error, the ratio is maintained at almost a constant value of about 1.7 over the entire concentration range at equivalent concentrations. At 5 °C, however, the value of the ratio increases with increasing concentration of polymer from 1.05 (at low concentrations of polymer) to 1.59 (at higher concentrations) over the entire concentration range. The values of the ratio, $\ln\gamma_{SOD}(Dex)/\ln\gamma_{SOD}(Fic)$ at 5 °C at low concentrations of polymers, suggest that at low temperature and in dilute solution, the energy cost of inserting a single SOD molecule in Dextran T70 is only marginally higher than that of inserting SOD into the same concentration of Ficoll 70. However, with increasing polymer concentration, the solvation energy of SOD in Dextran increased more rapidly than it does in Ficoll 70 of equivalent concentration. This finding appears like a contravention of the finding in the previous section, which indicates that even at low concentrations of each polymer, the solvation energy of Dextran T70 is almost twice that of the Ficoll 70 and that the self-interaction of each polymer species is temperature independent. To account for this seemingly strange observation, we postulate the following possibilities: (1) the high polymer–polymer repulsion between Dextran T70 molecules at low concentrations is less important to the solvation of SOD, because of the significantly smaller size of SOD compared with either Dextran T70 or Ficoll 70. (2) At low temperature, the attractive interaction between SOD and the polymer, which compensates for the repulsive interaction, is greater in the SOD–Dextran system than in the SOD–Ficoll 70 system. (3) Low temperature causes the presumed elastic Dextran T70 to shrink, thereby creating space within the solution for the solvation of SOD, thus, lowering the solvation energy of SOD in Dextran T70 at 5 °C compared to the solvation energy at higher temperatures.

An equally important question which remains to be answered is, "What is the reason for the increase in the value of the ratio $\ln\gamma_{SOD}(Dex)/\ln\gamma_{SOD}(Fic)$ with increasing polymer concentration, at low temperature?" We posit that since Dextran T70 has a more extended structure, at low temperature, it can trap SOD within its network of intermolecular matrix, thus inducing self-association of SOD. Such an effect is highly unlikely in Ficoll 70, since it is more compact and would be unable to trap SOD in its intra-molecular matrix. However, with increasing concentrations of polymers, at low temperatures, the dimerization of SOD increases the energy cost of inserting SOD dimers into Dextran T70 solution than into equivalent concentrations of Ficoll 70. Therefore, the free energy of insertion of SOD into Dextran T70 increases more rapidly with increasing concentration of Dextran T70 than with increasing Ficoll 70 concentration. Moreover, because of the more extended nature of Dextran T70, to accommodate SOD in a solution of a high concentration of Dextran T70, additional energy above that for Ficoll 70 is needed to create space and make the size of Dextran approach that of a hard particle. More and more of this energy is needed with increasing concentration of Dextran T70 (compare V_{eff} values of the polymers in Tables 1, 2). This observation could account for the higher value of the self-association constant of SOD in Dextran T70 (log $K^\circ_{S_2}$ (5 °C) = 2.23 corresponding to $K^\circ_{S_2} = 169.82$ dm^3 mol^{-1}) than in Ficoll 70 with log $K^\circ_{S_2}$(5 °C) = 1.97 corresponding to $K^\circ_{S_2} = 93.33$ dm^3 mol^{-1} (compare values of log $K^\circ_{S_2}$ in column 2 of Tables 1, 2). This conclusion is further justified by the significant improvement seen in the fitted curve when dimerization of SOD was allowed at 5 °C, using the hard convex particle model for the SOD–Dextran T70 system. It is noteworthy that in fitting, the experimental data at higher temperatures to the effective hard particle model, allowing for the variation of $K^\circ_{S_2}$, the SOD self-association term, in addition to K°_{SD}, the equilibrium constant of hetero-association did not result in a significant improvement of the fits to the experimental data. This is so for both the SOD–Ficoll 70 and SOD–Dextran T70 systems (compare SSR of Table 1, column 2, with that of Table 4, column 1; also compare SSR of Table 2, column 3, with that of Table 2, column 2). It is remarkable that the values of log $K^\circ_{S_2}$ in Table 4 are also negative. This suggests the absence of self-association at temperature > 5 °C. The implication of these findings is that the self-association of SOD which is unimportant above 5 °C becomes important in Dextran T70 at 5 °C.

Based on our experimental results, we rationalized the earlier experimental finding (Jiao et al. 2010) that SOD self-association at low temperatures might partly account for the

Table 4 Fitting parameters for binary mixtures of SOD and polymers with statistical model III permitting both self- and hetero-attractive interactions at all experimental temperatures

SOD in Dextran T70	SOD in Ficol70
$M^*_D = 21{,}664(-600, +880)$	$M^*_F = 22{,}996.781$
$M^*_S = 7679+, (-63+39)$	$M^*_S = 7658.9747$
$V_{\mathrm{eff},S} = 1.5522$	$V_{\mathrm{eff},S} = 1.4892$
$V_{\mathrm{eff},D} = 2.01$	$V_{\mathrm{eff},F} = 1.32$
$\log K^\circ_{S_2}(5\ ^\circ\mathrm{C}) = 2.20$	$\log K^\circ_{S_2}(5\ ^\circ\mathrm{C}) = 2.09$
$\log K^\circ_{S_2}(27\ ^\circ\mathrm{C}) = -1029.36$	$\log K^\circ_{S_2}(25\ ^\circ\mathrm{C}) = 1.76$
$\log K^\circ_{S_2}(37\ ^\circ\mathrm{C}) = -29{,}498.53$	$\log K^\circ_{S_2}(37\ ^\circ\mathrm{C}) = -1416.45$
$\log K^\circ_{SD}(5\ ^\circ\mathrm{C}) = 2.30$	$\log K^\circ_{SF}(5\ ^\circ\mathrm{C}) = 2.20$
$\log K^\circ_{SD}(27\ ^\circ\mathrm{C}) = 2.13$	$\log K^\circ_{SF}(25\ ^\circ\mathrm{C}) = 2.08$
$\log K^\circ_{SD}(37\ ^\circ\mathrm{C}) = 1.96$	$\log K^\circ_{SF}(37\ ^\circ\mathrm{C}) = 2.03$
$\mathrm{SSR} \times 10^{-8} = 1.2$	$\mathrm{SSR} \times 10^{-7} = 4.4$

Subscripts symbols and units are defined in Tables 1 and 2

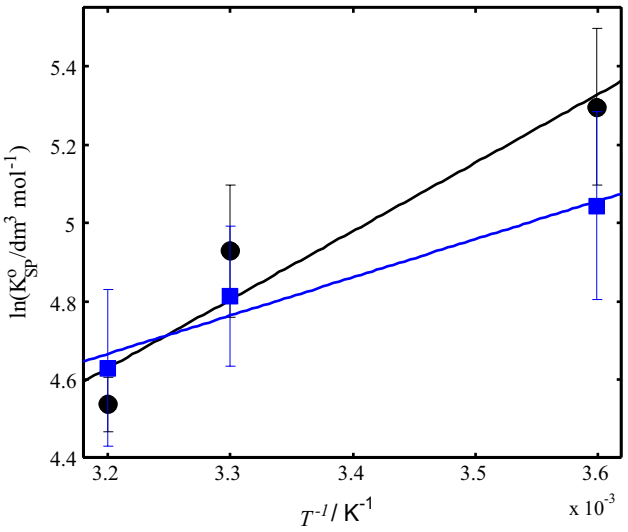

Fig. 4 Estimates of the temperature dependence of the equilibrium constant for the apparent "binding" of trace SOD with Dextran T70 (black circles and line), and SOD with Ficoll 70 (blue squares and line). Best-fit values of temperature dependent K°_{SP} obtained from fitting the effective hard convex particle model to the combined data at three temperatures (column 2 of Table 1 and column 3 of Table 2)

reduced binding of catalase to SOD at low temperatures and high polymer concentrations. Dimerization of SOD, which occurs at high polymer concentrations and low temperatures, should reduce the concentration of SOD monomers which are free to associate with catalase, thereby inhibiting association between SOD and catalase. This finding suggests the possibility of competition between SOD self-association and hetero-association between protein and polymer, depending on the temperature and on the concentration of the crowder. Like protein–polymer association, the self-association of SOD might also be temperature dependent. In view of the previous experimental results (Jiao et al. 2010) and other findings, one might assume that low temperatures of about 5 °C or less would preserve or promote the self-association of SOD molecules as well as hetero-association between SOD and polymer molecules. This discovery may be an important antecedent in identifying the temperature conditions under which trace proteins in crowded solutions could be stored if self-association is desirable, especially if the state of association is important in determining the activity of such proteins. The activities of proteins which dissociate in dilute solutions, but are active as dimers and oligomers may need to be preserved by storing them at low temperature in a high concentration of a polymeric additive such as Dextran T70.

This finding is consistent with the previous studies in that concentrated solutions of proteins as well as polymers have been shown to induce temperature-dependent attractive hetero-interaction (Minton 2001; Fodeke and Minton 2011; Jiao et al. 2010). It is also consistent with earlier findings, which demonstrated that the self-association of tubulin occurs in the presence of high concentrations of Dextran T70 (Rivas et al. 1999). It has also been previously reported that dextran concentration up to 0.09 g dm^{-3} caused aggregation of human red blood cells (Neu et al. 2008).

Thermodynamic consequences of the interactions

To determine the thermodynamic consequences of the temperature-dependent attractive hetero-interaction, the enthalpy and entropy of interaction of SOD with each of the polymers are obtained from Fig. 4.

The logarithm of K°_{ij} ($i = S$ and $j = D$ or F), the weak hetero-association constant at infinite dilution, obtained from parameters of the best-fit curve through the experimental data (Table 1, column 2, for the SOD–Dextran T70 system; Table 2, column 3, for the SOD–Ficoll 70 system), was plotted against the reciprocal of the temperature. The interaction of each of the polymers with SOD was exothermic, suggesting that the energies of the products are lower than the reactants in each case. The enthalpy of the interaction of SOD with Dextran T70 is ca. 1.75 times higher than that of its interaction with Ficoll 70. This result is in quantitative accord with the relative value of the free energy of interaction of Dextran T70 with SOD, which is between 1.6 and 1.9 times that of the interaction of Ficoll 70 with SOD. This might suggest that there is a strong correlation between the enthalpy of protein–polymer interaction and the free energy of insertion of protein into the carbohydrate polymer. The entropy change accompanying the interaction of SOD with Ficoll 70 in the limit of the low concentration of Ficoll 70 is > 0, signifying a net increase in entropy under these conditions. This suggests that in the limit of the low concentration, the net interaction between Ficoll 70 molecules and SOD molecules

leads to increased randomness in the solution. The entropy change accompanying the interaction between SOD and Dextran T70 is < 0, signifying a reduction in the entropy of interaction of SOD molecules with Dextran T70 at low polymer concentrations. This indicates that the weak attractive interaction between SOD and Dextran T70 molecules could be long range, and is significant enough to reduce the entropy of the solution. The structural and thermodynamic parameters obtained from SOD–Dextran T70 and SOD–Ficoll 70 systems are reported in Table 3 for comparison. It is significant to note that the fit of the structural convex hard particle model to the SOD–Dextran T70 data is not as good as the fit to the SOD–Ficoll 70 data. Attempts to use the Ogston model for the SOD–Dextran T70 data produced even a poorer fit to the experimental data (not shown). The difficulty with using the Ogston model for fitting the experimental data might be the consequence of the attractive interaction between molecules of SOD on one hand and between SOD and Dextran T70 molecules on the other hand. We, therefore, opted to quantify the total attractive interaction between molecules of SOD and the carbohydrate polymer molecules.

SOD–Dextran T70 attractive interaction

The solvation energy in a crowded solution has been separated into repulsive and attractive components (Kim and Mittal 2013). Using the calculated non-ideality factor, $\ln\gamma$ values, obtained from the best-fit values of B_{21} and B_{211}, the logarithm of the net values of the activity coefficient, $\ln\gamma_{net}$, due to the interaction between SOD and Dextran T70, is given by

$$\ln\gamma_{net} = \ln\gamma_{excluded} - \ln\gamma_{attractive}. \quad (18)$$

In Eq. (18), $\ln\gamma_{excluded}$ is the entropic term, which is independent of temperature and $\ln\gamma_{attractive}$ is the temperature-dependent term.

We posit that the deviation of the temperature-dependent curves of activity coefficient for the SOD–Dextran T70 system (black curves of Fig. 3b) from the Ogston model curve (red curve in Fig. 3b) arises from an attractive interaction between SOD and Dextran. Figure 5 shows the dependence of the hetero-attractive interaction on w_{Dex} calculated from Eq. (18).

The dependence of w_{Dex} of the contribution to the non-ideality factor due to the attractive interaction between SOD and Dextran T70 is presented in Fig. 5. This was calculated by subtracting $\ln\gamma_{net}$ from $\ln\gamma_{excluded}$. The following points are clear from Fig. 5. (1) The attractive interaction increases with increasing w_{Dex} to a maximum value and then begins to diminish after a critical value of w_{Dex}, C^* characteristic of that temperature. (2) At a given critical w_{Dex}, the deviation of the activity coefficient from that predicted by the

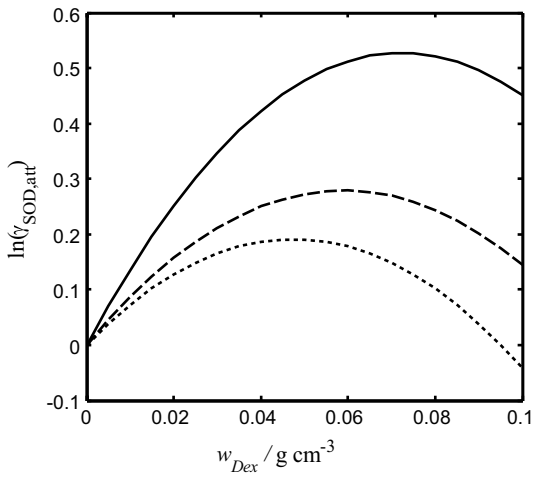

Fig. 5 Dependence of energy of attractive interaction between SOD and Dextran T70 on Dextran T70 concentration. Curve description: 5 °C, full curve; 27 °C, broken curve; 37 °C, dotted curve

excluded volume is maximum (the attractive interaction is maximum). (3) Attraction increases with decreasing temperature. Hence, the maximum value of the energy of attraction increases with decrease in temperature. (4) The critical values of w_{Dex}—w_{Dex} at maximum attraction—are ca. 0.07, 0.06, and 0.05 g cm^{-3} at 5, 27, and 37 °C, respectively. This suggests that C^* of Dextran T70 decreases with increasing temperature and that low temperature enhances attractive interactions. The observed critical property of Dextran T70 may have a strong relationship with earlier report (de Gennes 1979) which suggests that Dextran polymer molecules may exist in two conformations. According to de Gennes (1979), at low concentrations, the polymer is in a coil conformation with a specific radius of gyration. Above the critical overlap concentration, C^*, the polymer molecules form a polymeric network with a characteristic mesh size. For Dextran T70, this critical overlap concentration was reported to be 0.031 g cm^{-3} (Barshtein et al. 1998). It is not unlikely that the critical values of w_{Dex} (0.07, 0.06 and 0.05 g cm^{-3} at 5, 27, and 37 °C, respectively) have a relationship with the critical overlap concentration. This would then mean that the critical overlap concentration of a polymer such as Dextran T70 depends on temperature. That the critical concentration is highest at 5 °C and lowest at the highest temperature is an indication that the mesh size of the Dextran T70 polymer network is smallest at 5 °C and highest at the highest temperature. The difference in the value of C^* reported by Barshtein et al. (1998) and our values could arise from difference in the temperature, ionic strength of the medium, and/or the fact that the Dextran T70 used by the group contains no other molecules. It is, nonetheless, gratifying that their finding is also evident in the report here presented. Similarly, other researchers (Rad

et al. 2009; Neu et al. 2008) have demonstrated that in a system of human red blood cells (RBC) in ≤ 0.09 g cm^{-3} Dextran, the magnitude of RBC mobility decrease is significantly less than estimated for the corresponding increase in viscosity. The higher mobility relative to increased viscosity from the experiments, which were carried out at 25 °C in 0.005 and 0.015 (mol dm^{-3} NaCl), was accounted for in terms of reduced viscosity within the Debye–Huckel ionic atmosphere and development of polymer depletion (Rad et al. 2009). We suggest that the Dextran depletion might be due to the formation of a network of inter- and intra-molecular crosslinks with increasing w_{Dex}, a process which climaxes at C^*. It is interesting to note that in the work of Rad et al. (2009), the mobility of RBC in Dextran first increases steadily with increasing w_{Dex}, and then starts to increase more markedly at concentrations above 0.05 g cm^{-3}, in agreement with our findings. The process was also accompanied by RBC aggregation, which increases with increasing concentration of Dextran. We submit that the polymer depletion at the surface of the protein at the critical concentration, C^*, of Dextran may also account for the reduction in the $\gamma_{\mathrm{attractive}}$ due to attractive interaction between the polymer and the protein above C^*. The heavy crosslinks within Dextran T70 above C^* makes it behave more as a hard particle. This is an indication that above C^*, the attractive interaction between SOD and Dextran T70, which promotes hetero-association as against dimerization, is diminished and the interaction arises essentially from the excluded volume. To see if both the phenomena of depletion of high molecular weight Dextran on surface of RBC leading to aggregation occur by the same mechanism as the dimerization of SOD, an interesting experiment would be to study the SOD interaction in arbitrary concentrations of Dextran with a molecular weight significantly greater than 70 kDa. Lower value of C^* would suggest similar mechanism. The experiment reported by Rad et al. (2009) may also be carried out at temperatures below or above 25 °C. It is expected that C^* value would be > 0.05 g cm^{-3} (the value reported at 25 °C) but < 0.05 g cm^{-3} at temperature higher than 25 °C.

The marked overestimation of the effect of Dextran viscosity by the Helmholtz–Smoluchowski relation, with the difference increasing with Dextran molecular mass in agreement with the concept of polymer depletion near the RBC surface was also accounted for in terms a "depletion model" mechanism for dextran-mediated RBC aggregation. On our part, we quantified $\gamma_{\mathrm{attracive}}$ (the activity coefficient contribution due to attractive interaction between SOD and Dextran T70) by subtracting γ_{total} (activity coefficient in the presence of attractive interaction, obtained from model-free interaction parameters) from $\gamma_{\mathrm{excluded}}$ (the activity coefficient due to excluded volume using the Ogston model for which structural parameters were obtained from the hard particle model). Though the solubility of Dextran T70 at 25 °C is greater than 0.2 g cm^{-3}, the concentration of Dextran T70 used in our experiment was limited to 0.1 g cm^{-3}. Rad et al. had previously measured the viscosity corrected electrophoretic mobility of human RBC in dextran at concentrations up to 0.09 g cm^{-3}, a value greater than the reported C^* at all temperatures of the experiment.

Conclusion

Using the convex hard particle model, it was possible to show that the attractive interactions between polymer molecules and SOD molecule are important in both carbohydrate polymers at all temperatures of the experiment. At low temperature, self-association leading to dimerization of SOD, which is insignificant in Ficoll 70, becomes important in Dextran T70. This is an indication that the structure of the polymer and temperature conditions play a critical role in determining the type and extent of interaction which occurs in a binary crowded solution. An important finding in this work is in quantifying self- and hetero-attractive interactions between protein and Dextran T70, for which structural model had remained unresolved. The attractive interaction increases with reduction in temperature and with an increase in the concentration of the carbohydrate polymer until the critical concentration is attained. After the critical concentration, the attractive interaction between protein and Dextran T70 begins and continues to diminish, the polymer approach hard particle with increasing concentration. The reliability of the result of this experiment lies in the agreement between the fit of the experimental data to model-free virial expansion of the activity coefficient and the result of the structural hard particle model. We postulate that the Ogston model was unable to account for the interaction between Dextran T70 and SOD, due to the attractive interaction between SOD and Dextran T70, on one hand, and the high tendency of Dextran T70 to induce significant self-association of the protein. It would, however, be interesting to determine how the concentration of a protein such as SOD affects its self-association at a constant concentration of Dextran T70.

Acknowledgements The author thanks Dr. A. P Minton for making the facilities in his laboratory available for this work and for useful suggestions. The author is also grateful to Prof. K.O. Okojo for proofreading the manuscript.

Appendix

To demonstrate the relative importance of self-association (dimerization) of SOD involving $K^{\circ}_{S_2}$ and K°_{SD} at low temperature, we fitted the data of SOD in Dextran T70 at 5 °C allowing for the variation of only one of the two

interaction parameters. In Fig. 6, the fitted curve to the experimental data for the dependence M^*_{SOD} on w_{Dex} at 5 °C (Fig. 1b) with the best-fit value of $K^\circ_{S_2}$ at 5 °C, neglecting hetero-association is presented along with the fitted curve with best-fit value of K°_{SD} at 5 °C, neglecting self-association. The calculated curve using the fitting parameters of both K°_{SD} and $K^\circ_{S_2}$ of Table 1 (column 2) of the convex hard particle model at 5 °C is also plotted for comparison. It is seen that while the curve calculated with best-fit values of both K°_{SD} and $K^\circ_{S_2}$ is very good, neither the curve calculated with best-fit value of K°_{SD} or $K^\circ_{S_2}$ alone produced good fit to the experimental data. The worse fitting curve to the data (dotted curve) is that in which the hetero-association between SOD and Dextran T70 was "switched off" leaving only the self-association of SOD. The SSR obtained was 11 times greater than that which allows for only hetero-association between Dextran T70 and trace SOD. This shows that under the experimental conditions, whereas weak hetero-association is important at all temperatures, weak self-association becomes important only at low temperature. It also shows that the weak attractive interaction between SOD and polymer molecules is more important than protein self-association under the conditions of the experiment. The result obtained in the SOD–Dextran system is qualitatively similar to the finding for the interaction of SOD with Ficoll 70, except that in the SOD–Ficoll 70 system, the value of the equilibrium constant for the self-association of SOD is somewhat lower. The result also suggests that even at low temperature, the hetero-association term is more important in describing the phenomenon of the interaction between Dextran T70 molecules and SOD than self-association of SOD molecules.

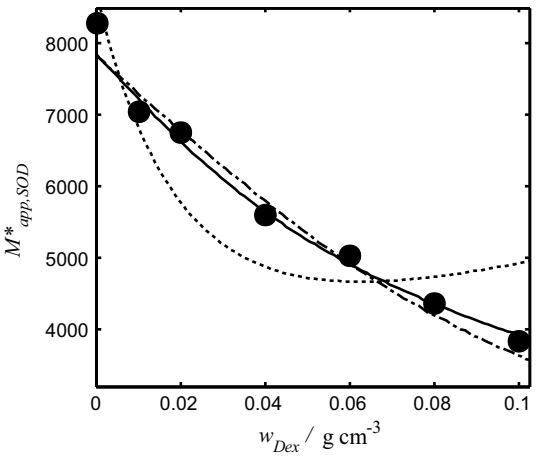

Fig. 6 Experimental data points of apparent buoyant molar mass of SOD as a function of *w/v* concentration of Dextran T70 at 5 °C, fitted to the convex hard particle model assuming both hetero-association between Dextran T70 and SOD and self-association of SOD (full curve); only self-association of SOD (dotted curve); and only hetero-association of SOD with Dextran T70 (broken-dotted curve). Each experimental data point is the mean of at least two replicate experiments subject to about 5% standard error

References

Barshtein G, Tamir I, Yedgar S (1998) Red blood cell rouleaux formation in dextran solution: dependence on polymer conformation. Eur Biophys J 27:177–181

Boublik T (1974) Statistical thermodynamics of convex molecule fluids. Mol Phys 27:1415–1427

Darawshe S, Rivas G, Minton AP (1993) Rapid and accurate microfractionation of the contents of small centrifuge tubes: application in the measurement of molecular weights of proteins via sedimentation equilibrium. Anal Biochem 209:130–135

de Gennes PG (1979) Scaling concepts in polymer physics. Cornell University Press, Ithaca

Ellis RJ (2001) Macromolecular crowding: obvious but underappreciated. Trends Biochem Sci 26:597–604

Fodeke AA, Minton AP (2010) Quantitative characterization of polymer–polymer, protein–protein, and polymer–protein interaction via tracer sedimentation equilibrium. J Phys Chem B 114:10876–10880

Fodeke AA, Minton AP (2011) Quantitative characterization of temperature-independent and temperature-dependent protein–protein interactions in highly-nonideal solutions. J Phys Chem B 115:11261–11268

Fulton AB (1982) How crowded is the cytoplasm? Cell 30:345–347

Homouz D, Perham M, Samiotakis A, Cheung MS, Stafhede WP (2008) Crowded, cell-like environment induces shape changes in aspherical protein. Proc Natl Acad Sci 105(33):11754–11759

Jiao M, Li H-T, Chen J, Minton AP, Liang Y (2010) Attractive protein–polymer interactions markedly alter the effect of macromolecular crowding on protein association equilibria. Biophys J 99:914–923

Kim YC, Mittal J (2013) Crowding induced entropy-enthalpy compensation in protein association equilibria. Phys Rev Lett 110:208102-1–208102-5

Labowitz JL, Helfand E, Praestgaard E (1965) Scaled particle theory of fluid mixtures. J Chem Phys 43(3):774–779

Laurent TC, Killander JA (1964) Theory of gel filtration and its experimental verification. J Chromatogr A 14:317–330

McMillan WG, Mayer JE (1945) The statistical thermodynamics of multicomponent systems. J Chem Phys 13:276–305

Minton AP (1983) The effect of volume occupancy upon the thermodynamic activity of proteins: some biochemical consequences. Mol Cell Biochem 55:119–140

Minton AP (2001) The influence of macromolecular crowding and molecular confinement on biochemical reactions in physiological media. J Biol Chem 276:10577–10580

Mukherjee S, Waegele M, Chowdhury LG, Gai F (2009) Effect of macromolecular crowding on protein folding dynamics at the secondary structure level. J Mol Biol 393:227–236

Neu BJ, Wenby R, Meiselman HJ (2008) Effects of dextran molecular weight on red blood cell aggregation. Biophys J 95:3059–3065

Ogston AG (1958) The spaces in a uniform random suspension of fibers. Trans Faraday Soc 54:1754–1757

Ogston AG (1970) On the interaction of solute molecules with porous networks. J Phys Chem 74:668–669

Rad S, Gao J, Meiselman HJ, Baskurt OK, Neu B (2009) Depletion of high molecular weight dextran from the red cell surface measured by particle electrophoresis. Electrophoresis 30:450–456

Rivas G, Fernandez JA, Minton AP (1999) Direct observation of the self-association of dilute proteins in the presence of inert macromolecules at high concentration via tracer sedimentation equilibrium: theory, experiment, and biological significance. Biochemistry 38:9379–9388

Rosen J, Kim YC, Mittal J (2011) Modest protein-crowder attractive interaction can counteract enhancement of protein association by intermolecular excluded volume interaction. J Phys Chem 115:3683–3689

Zimmerman SB, Minton AP (1993) Macromolecular crowding: biochemical, biophysical, and physiological consequences. Annu Rev Biophys Biomol Struct 22:27–65

Zimmerman SB, Trach SO (1991) Estimation of macromolecule concentrations and excluded volume effects for the cytoplasm of *Escherichia coli*. J Mol Biol 222:599–620

Zorrilla S, Jiménez M, Lillo P, Rivas G, Minton AP (2004) Sedimentation equilibrium in a solution containing an arbitrary number of solute species at arbitrary concentrations: theory and application to concentrated solutions of ribonuclease. Biophys Chem 108:89–100